# Quantitative Distribution of GABA-immunopositive and -immunonegative Neurons and Synapses in the Monkey Striate Cortex (Area 17)

C. Beaulieu,[1,2,3] Z. Kisvarday,[2,4] P. Somogyi,[2] M. Cynader,[3] and A. Cowey[4]

[1] Department of Pathology, Université de Montréal, Montréal H3C 3J7, Canada, [2]MRC Anatomical Neuropharmacology Unit, Oxford University, Oxford OX1 3TH, United Kingdom, [3] Department of Ophthalmology, University of British Columbia, Vancouver V5Z 3N9, Canada, and [4] University Department of Experimental Psychology, Oxford OX1 3UD, United Kingdom

**The number of GABA-immunoreactive [GABA(+)] neurons and synapses was determined in functionally distinct subregions delineated as rich and poor in cytochrome oxidase (CO) in the visual cortex of adult macaque monkeys. The average numerical density (number per unit volume, $N_v$) of GABA(+) neurons and synapses was not significantly different between the CO-rich and -poor regions. Twenty percent of the total number of cortical neurons and 17% of the synapses were GABA(+). On average, each visual cortical neuron receives 3900 synapses, 660 of them being GABA(+). The latter were distributed on the target cell in a pattern that predicts the site of GABA influences in cortex. The major targets of GABA(+) synapses were dendritic shafts, comprising nearly two-thirds of the postsynaptic elements. About every fourth and every eighth GABA(+) synapse was devoted to dendritic spines and to neuronal somata, respectively. Axon initial segments, although the exclusive targets of GABA(+) cells, comprise less than 0.1% of structures postsynaptic to GABA(+) boutons. From this distribution, we estimate that in each cubic millimeter of striate cortex there were about 20 million GABA(+) synapses on dendritic spines, 47 million on dendritic trunks, 9 million on somata, and fewer than 0.1 million on axon initial segments.**

**The sites of influences of GABA-immunonegative [GABA(−)] synapses were different in that they target mainly dendritic spines and dendritic trunks. About two-thirds of GABA(−) synapses were on dendritic spines, and the remainder were devoted to dendritic trunks. Only a minute fraction innervate somata. We estimate that in 1 mm$^3$ of striate cortex there were about 235 million GABA(−) synapses on spines, 133 million on dendrites, and about 2 million on somata. The proportions of GABA(+) neurons and synapses and their target distribution did not appreciably differ from those of the visual cortex of the cat even though the numerical density of neurons was 2.5 times higher in the monkey.**

A description of the circuitry of the cerebral cortex requires the determination of quantitative synaptic relationships. Establishing indices of convergence, divergence, and the chemical status of cells and synapses are all central in constructing valid models of the cerebral cortex. In addition, these characteristics must be estimated separately in different cortical laminae because of their specific connectivity. The location of a synapse on the surface of the neuron may greatly influence its effect; therefore, the quantitative data should ideally include the distribution of synapses on different portions of the recipient cells.

GABA is considered to be the major inhibitory neurotransmitter in the cerebral cortex (Krnjevic, 1984), contributing to several specific response properties of neurons in the visual (Sillito, 1975, 1977; Sillito et al., 1980) and in the somatosensory cortex (Dykes et al., 1984). Most of the GABA in the cortex is synthesized and released by intrinsic cortical neurons, which show great anatomical variation. Although the anatomical localization of GABA synapses has been studied in different areas of the primate cerebral cortex (Houser et al., 1984; Kisvarday et al., 1986), there is only sparse information on the overall distribution of GABA-positive and GABA-negative [GABA(+), GABA(−), respectively] synapses. One reason for this is that previous immunohistochemical studies for markers such as glutamate decarboxylase (GAD) or GABA could only demonstrate the pattern of GABAergic innervation qualitatively; technical limitations have prevented the determination of the number, density, and proportion of GABAergic synapses. In a recent study, the quantitative distribution of GABA(+) synapses was determined for the first time in the cat visual cortex (Beaulieu and Somogyi, 1990), using an immunogold technique.

In the present study, the quantitative distribution of GABA(+) neurons and synapses was estimated in the different laminae of the visual cortex (area 17) of macaque monkey. This was made separately in the cytochrome oxidase (CO)-rich and -poor regions of area 17. In addition, targets of GABA(+) synapses were estimated in order to quantify the major sites of GABA influence in the monkey's primary visual cortex.

## Materials and Methods

Tissue was obtained from four adult monkeys (three *Macaca mulatta,* animals A, B, D; and one *Macaca*

*fascicularis,* animal C), which were used for the localization of a number of neuroactive substances and corticocortical projections. At the end of the tracer experiments, animals received a lethal intravenous dose of sodium pentobarbitone and were perfused through the heart first with 500–800 ml of Tyrode's solution (gassed continuously with 95% $O_2$, 5% $CO_2$ mixture) followed by 4 liters of fixative containing 1.5% paraformaldehyde (TAAB Co.) and 1–2% glutaraldehyde (TAAB Co.) in 0.1 M phosphate buffer (PB), pH 7.4. After perfusion, the brain was removed and kept in fixative for a few hours followed by several washes in 0.1 M PB.

### *Tissue Processing*

Serial sections (60–80 μm thick) of large blocks of the visual cortex were cut parasagittally on a vibratome, washed thoroughly in PB (pH 7.4), and stored in the same buffer overnight, at 4°C. Alternate sections were processed either for electron microscopy (EM) or for CO staining using the protocol of Wong-Riley (1979) modified by Silverman and Tootell (1987). Briefly, the sections were rinsed in a washing medium of 0.1 M PB (pH 7.6) containing 10% sucrose for 4 × 10 min and transferred into 0.05 M Tris buffer (TB; pH 7.6) solution containing 275 mg/liter cobalt chloride, 10% sucrose, and 0.1% Triton X-100 (omitted when sections were processed for EM), for 10 min. After 2 × 5 min washes in PB, incubation of the sections was carried out in 0.1 M PB containing 50 mg of 3,3′-diaminobenzidine tetrahydrochloride (Sigma), 5 gm of sucrose, 7.5 mg of cytochrome C (type III; Sigma), 2 mg of catalase per 100 ml, and 0.1% Triton X-100 (omitted for EM) under constant agitation at 38–39°C for 4–9 h. The sections were then washed thoroughly in PB. They were mounted on chrome–gelatin-coated slides and covered with a mounting medium under a coverslip for light microscopic observations. Sections for EM were washed in PB, postfixed for 30 min in 1% osmium tetroxide dissolved in 0.1 M PB (pH 7.4), dehydrated, and embedded on glass slides in Ducurpan ACM (Fluka) resin. In animal D, CO-stained sections were processed for EM, osmium treated (1% in PB 0.1 M, 30 min), and mounted on glass slides in resin.

For EM, ribbons of area 17 extending from the pia to the white matter were cut out from the osmium-treated sections of the slides and reembedded in resin. Guided by the pattern of CO staining in layer II-III of neighboring sections or directly on the osmium-treated section, each ribbon was trimmed so that the longitudinal edges were perpendicular to the pia and to the white matter, and enclosed to the radial axis of either a CO-rich or -poor region. Layering of the cortex was determined in osmium-treated and consecutive CO-reacted sections using Lund and Boothe's (1975) classification scheme.

### *Determination of the Number and Proportion of GABA(+) Neurons*

The numerical density of neurons (number per unit volume, $N_V$) was calculated in each lamina of the monkey visual cortex and separately in CO-rich and CO-poor regions in three of the four animals (animals A, C, and D). Series of 5–10 semithin sections extending from the pia to the white matter were cut for each block. In order to localize the GABA(+) neurons, alternate sections were either reacted with the postembedding method using the protocol as described by Somogyi and Hodgson (Somogyi et al., 1985) or stained with azure–methylene blue (Fig. 1; Richardson et al., 1960).

The numerical density of neurons per unit volume ($N_V$) was calculated in each cortical lamina (layers I, upper and lower half of II-III, IVA, IVB, upper and lower half of IVC, V, and upper and lower half of VI) by stereological methods, as detailed by Colonnier and collaborators (O'Kusky and Colonnier, 1982; Beaulieu and Colonnier, 1983, 1985b). The neuronal nuclei were used as test objects because of their regular shape. All neuronal nuclei present in a 100-μm-wide strip of methylene blue–stained tissue were drawn from the pia to the white matter. Altogether, 6–10 nonoverlapping strips were analyzed in each animal. Immunoreactive neurons were then determined using adjacent sections reacted for the demonstration of GABA.

The numerical density ($N_V$) of neurons was calculated according to the formula for ellipsoids (Weibel, 1979):

$$N_V = \frac{K \times (N_A)^{1.5}}{\beta \times (V_V)^{0.5}}$$

where $N_A$ is the number of profiles per unit area; $V_V$ is the total volume of the objects divided by the total tested volume of the specimen, and this was equal to the total area of profiles divided by the total sampled area; $K$ is a factor derived from the size distribution of the test objects; and $\beta$ is a function of the axial ratios of the ellipsoids studied. The areas and the major and minor axes were obtained by direct measurement of the nuclear profiles on an electromagnetic graphic tablet, and yielded $V_V$ and $\beta$. For biological objects, $K$ rarely exceeds 1.1 but will most often be in the range of 1.01–1.1 (Weibel, 1979). We ascribed a value of 1.05 to $K$, and this gave an $N_V$ value corresponding closely to that obtained using a nucleolar count with an Abercrombie correction (Beaulieu and Colonnier, 1983). The number of neurons per unit column ($N_C$) was calculated by multiplying the $N_V$ of each lamina by the thickness of the lamina determined directly on the methylene blue–stained section with the help of the CO-reacted section.

The numerical density of neurons was obtained also by using the disector method (Sterio, 1984). The principles underlying this method of quantification do not rely on assumptions about the shape or the size–frequency distribution of the test objects as does the method mentioned above. The disector method uses two parallel sections separated by a known distance (Sterio, 1984). Profiles present on one section (reference section) and disappearing on the serial "look-up" section were counted according to the following formula:

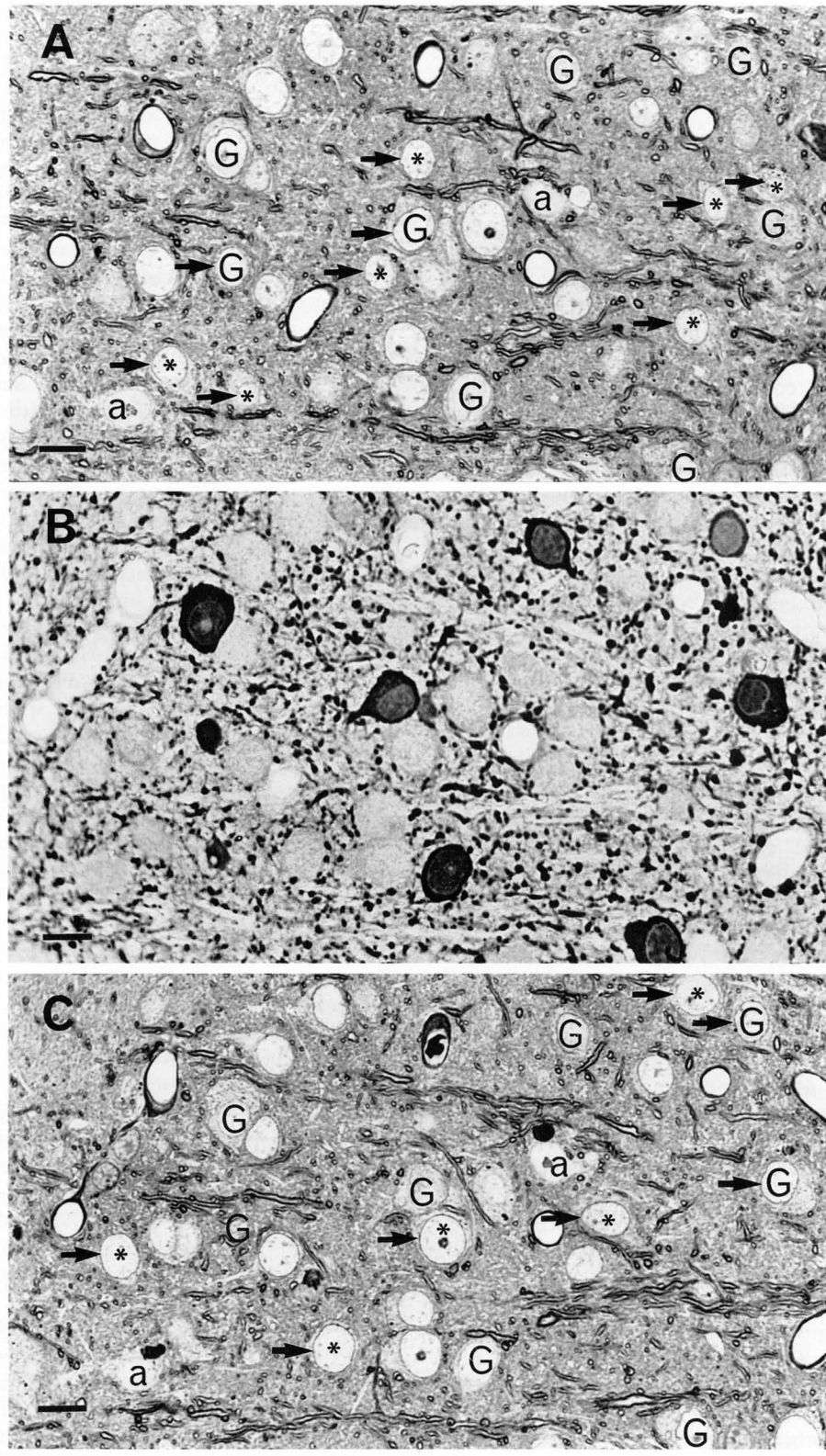


**Figure 1.** Light micrographs of three serial semithin sections taken in layer III of monkey visual cortex. *A* and *C* are from sections stained with azure–methylene blue, while *B* is from a section reacted for the demonstration of GABA. *Arrows* indicate nuclear membranes of neurons that are not found on the serial azure–methylene blue section. *Asterisks* indicate the nuclei of GABA(−) neurons not present in the serial azure–methylene blue section. *G*, GABA(+) neurons; *a*, astrocytes. Scale bars, 20 μm.

$$N_V = \frac{\Sigma\, Q-}{a \times h}$$

where $Q-$ is the number of nuclei appearing in the test area of the reference section but absent in the look-up section. The volume reference corresponds to the area sampled ($a$) multiplied by the distance ($h$) between the two sampling sections (the disector).

As described above, series of semithin sections were

cut and alternate sections were reacted for the demonstration of GABA. All neuronal nuclei present in a 100 μm strip of tissue in a section of the series were drawn from the pia to the white matter. For a comparison of the two methods, we used the same drawings analyzed with the previous method. The presence of the neuronal nuclei profiles was then checked two sections ahead in the series that was stained with methylene blue. All profiles that disappeared or were absent on the first section were recorded. Immunoreactivity for GABA was verified in the adjacent sections of the series.

For the determination of the distance between the reference and look-up sections, the section thickness has to be measured precisely. The ultramicrotome (Ultracut E) was set to 0.99 μm, and many series of 100 sections from five blocks of tissue were cut. The initial and the final thicknesses of the blocks were determined using a precise digital micrometer (Digitrix II). The estimated mean thickness of each section was 0.95 ± 0.04 μm. This estimate was also regularly checked throughout the experiment on shorter series and was found to be consistent. We therefore used this value for the mean thickness of each semithin section. Since the reference and the look-up sections were separated by two sections, the value of $h$ in the disector formula was 1.90 μm.

### *Quantitative Analysis of GABA(+) Profiles in EM Sections*

To determine the number of GABA(+) elements in CO-rich and -poor regions, ultrathin sections were mounted onto single-slot nickel grids and reacted with an antiserum to fixed GABA using a postembedding colloidal gold method (Somogyi and Hodgson, 1985). Briefly, the sections were treated with 1% periodic acid and 1% sodium periodate to etch the resin and remove the osmium. After washing, the grids were sequentially placed on drops of 1% ovalbumin, rabbit anti-GABA serum [Hodgson et al., 1985; code no. 9, diluted 1:1000 in Tris-buffered saline (TBS)], 0.1% polyethylene glycol in TB (pH 7.4), colloidal gold (15 nm) coated with goat anti-rabbit IgG (Bioclin; diluted 1:20 to 1:40 in the previous solution). Between these steps, the grids were washed in TBS. Finally, they were washed in filtered distilled water, air dried, exposed to osmium vapor for 1 min, stained with saturated uranyl acetate for 10–20 min, and contrasted with a fresh solution of lead citrate.

To test the specificity of the immunocytochemical method, some sections were incubated in the full sequence of reagents except that the antiserum to GABA was replaced with the same dilution of normal rabbit serum. Other sections were incubated in the anti-GABA serum that was previously preadsorbed to conjugated GABA using a solid-phase procedure (Hodgson et al., 1985). No selective gold or peroxidase labeling (on semithin sections) was observed under these conditions. The antiserum to GABA showed a small cross-reactivity with β-alanin and γ-amino-β-hydroxybutyrate; singular of those compounds is known to be concentrated in neurons. Therefore, their possible presence in the sections should not affect the results.

In each animal, 10 nonoverlapping micrographs (covering about 400 $\mu m^2$) were taken at a magnification of 14,000× in each cortical lamina (layers I, II-III, IVA, IVB, IVC, V, and VI). In three of the four animals, data were collected separately for CO-rich or -poor regions. All negatives were printed at a final magnification of approximately 30,000×.

The numbers of synapses were counted and lengths of synaptic contacts were measured on an electromagnetic tablet. A synapse was defined as the apposition of two profiles, one of which contained synaptic vesicles adjacent to a differentiated presynaptic membrane. Occasionally, two or three small zones of synaptic membrane thickening occurred between a pre- and postsynaptic profile. In studies using reconstruction of synapses from serial sections, it has been shown (Peters and Kaisermann-Abramof, 1969; Cohen and Siekevitz, 1978) that these actually correspond to a single "perforated" synaptic junction. Such synaptic appositions were thus taken as a single synapse rather than two or three small ones.

Postsynaptic elements were classified under four different categories (Fig. 2). Dendritic shafts were identified by the presence of mitochondria and microtubules. In contrast, dendritic spines lacked mitochondria and microtubules, were of small diameter, and occasionally contained a spine apparatus. If the nucleus was absent on the print, somata were identified on the basis of their size and the high density of cell organelles such as Golgi apparatus. Axon initial segments were the most difficult postsynaptic elements to differentiate from dendritic shafts. Postsynaptic profiles were placed in this category on the basis of the presence of an undercoating beneath the plasma membrane and microtubule fascicles within the profiles (Fig. 2*A*, ais).

The immunoreactivity for GABA was qualitatively evaluated. Pre- and postsynaptic profiles were considered to be immunoreactive for GABA, if the density of gold particles was several times higher than that observed over nearby neuropil elements (e.g., Fig. 2, b+, d+). When the difference in the density of GABA immunogold labeling was not high enough to classify its GABA content unequivocally, it was placed in a category of "GABA-equivocal." It is assumed that the proportion of GABA(+) profiles in the category of the GABA-equivocal category was similar to that calculated for the identified contacts. Therefore, the numbers obtained for this category were added proportionally to the population of genuine GABA(+) synapses. Some of the postsynaptic elements could not be identified, and they were placed in the category of "unidentified postsynaptic elements." In the tables and figures that follow, the percentages of synapses on spines, dendritic trunks, and somata are percentages of postsynaptic elements that were unequivocally identified.

The numerical density of synapses (number per unit volume, $N_V$) was calculated using a method of size–frequency distribution, according to the formula

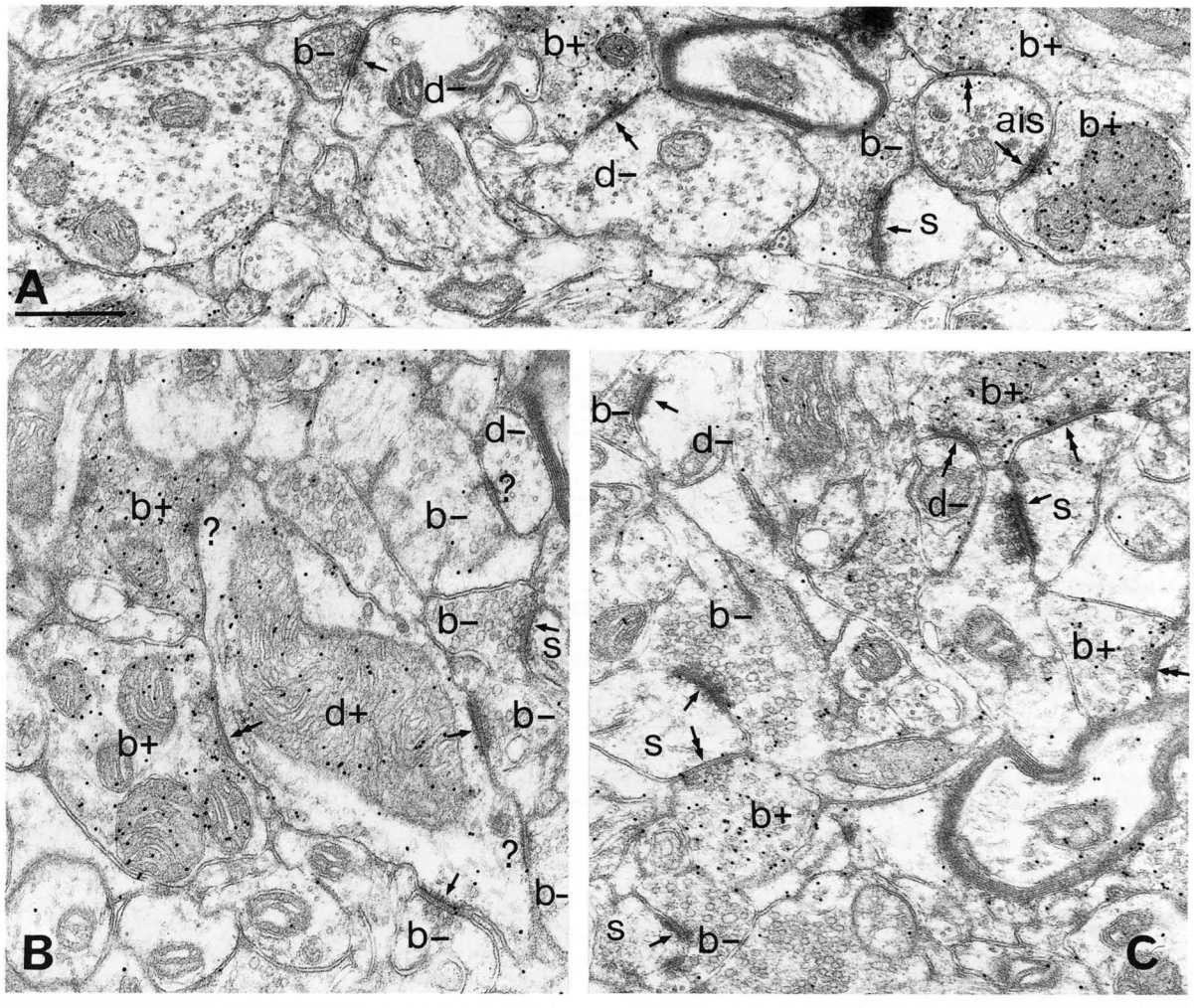


**Figure 2.** Electron micrographs of synaptic elements in the neuropil of layer III (*A*), layer IVC (*B*), and layer IVB (*C*) in the striate cortex of monkey. Sections were immunoreacted for GABA; profiles with high density of colloidal gold particles (e.g., *b+*, *d+*) are considered GABA(+). Gray's type 1 (*single arrows*) and type 2 (*double arrows*) synapses are found between immunopositive (+) and immunonegative (−) boutons (*b*), dendrites (*d*), spines (*s*), and axon initial segment (*ais*). The axon initial segment can be identified on the basis of fasciculated microtubules seen in cross section. Some synapses (*?*) cannot be classified in the section shown in *B*. Scale bar, 0.5 μm for *A–C*.

$$N_V = N_A / d$$

where $N_A$ is the number of synaptic contacts per unit area and $d$ is the mean trace length of the synaptic membranes. We used this formula because an empirical verification has shown that it was accurate for synaptic contacts of the size and shape that were found in 60–80 nm sections of cat cortex (Colonnier and Beaulieu, 1985).

In animal A, in addition to the above methodology, we applied the disector method for determining the number of synaptic contacts (Sterio, 1984; see review by Gundersen et al., 1988a,b). Two adjoining ultrathin sections were chosen, and overlapping electron micrographs from one section were taken from the pia to the white matter along the edges of sections representing the long axis of CO-rich and -poor regions. All synapses that were present in one section but disappeared in the other were counted. Because of the low number of test objects obtained with this method, only the total number of synapses was estimated: no attempts were made to classify these synapses in the different categories mentioned earlier. The numerical density of synapses was calculated using the disector formula given above for the estimation of neurons. The section thickness was determined by the single fold method (Weibel, 1979). The thickness of an ultrathin section was taken as equal to half the width of the smallest fold found. The thickness of each section was measured in different regions and the values were averaged to obtain a reliable estimate.

No direct estimate of tissue shrinkage was made. However, Colonnier and his colleagues (O'Kusky and Colonnier, 1982; Beaulieu and Colonnier, 1983) reported that the linear shrinkage of tissue taken from cat and monkey visual cortex and processed for EM was in the order of 14–16%. Therefore, we used a shrinkage value of 15%. It should be noted that the absolute values were affected by the shrinkage, and they were corrected accordingly. Nevertheless, the relative values such as the proportion of GABA(+) neurons and synapses, the number of GABA(+) synapses per neuron, and the relative distribution of synaptic targets among cortical laminae were independent of any tissue shrinkage.

**Table 1**
Comparison of different numerical data between CO-rich and CO-poor regions of monkey striate cortex

| | CO rich | CO poor |
|---|---|---|
| A. GABA(+) elements | | |
| $N_v$ neurons (thousand/mm³) | 21.4 ± 2.1 | 23.9 ± 1.6 |
| $N_v$ synapses (million/mm³) | 74 ± 5 | 77 ± 8 |
| Synaptic junction length (μm) | 0.25 ± 0.02 | 0.24 ± 0.03 |
| Targets | | |
| Spines (%) | 27.7 (0) | 25.7 (0) |
| Dendrites (%) | 58.7 (11.9) | 64.2 (5.9) |
| Somata (%) | 13.6 (0) | 10.1 (1.5) |
| B. GABA(−) elements | | |
| $N_v$ neurons (thousand/mm³) | 91.2 ± 3.1 | 97.2 ± 8.1 |
| $N_v$ synapses (million/mm³) | 335 ± 31 | 387 ± 27 |
| Synaptic junction length (μm) | 0.30 ± 0.02 | 0.30 ± 0.02 |
| Targets | | |
| Spines (%) | 64.3 (0.03) | 63.1 (0) |
| Dendrites (%) | 35.5 (8.8) | 36.3 (9.3) |
| Somata (%) | 0.3 (0.3) | 0.6 (0.6) |
| C. GABA(+) synapses in layer III of monkey C | | |
| $N_v$ (million/mm³) | 85 ± 8 | 88 ± 16 |
| Synaptic junction length (μm) | 0.29 ± 0.05 | 0.27 ± 0.02 |
| Targets | | |
| Spines (%) | 19.8 (0) | 29.2 (0) |
| Dendrites (%) | 65.6 (9.3) | 64.2 (6.9) |
| Somata (%) | 14.6 (2.1) | 6.6 (0) |

These data show the number of neurons and synapses per unit volume of tissue ($N_v$), synaptic length, and postsynaptic targets of GABA(+) (section A) and GABA(−) (section B) synaptic boutons in CO-rich or -poor columns of the total cortical depth (layers I–VI) of monkey striate cortex (means and SEM values; $n = 3$, animals A, C, and D) and in layer III of animal C (section C). Numbers in parentheses represent the proportion of GABA(+) postsynaptic targets.

## Results

### *Comparison of CO-Rich and -Poor Regions*

The numerical density ($N_v$) of neurons and synapses, synaptic length, and distribution on postsynaptic elements were analyzed separately in CO-rich or -poor regions in the visual cortices of three monkeys (animals A, C, and D). When comparing these different estimates, the results are similar in the two regions (Table 1). Indeed, percentage differences in neuronal or synaptic $N_v$, length of synaptic junctions, or distribution on postsynaptic elements of GABA(+) or GABA(−) synapses between CO-rich and -poor regions were usually low, and the values were not statistically different on a one-way ANOVA. In order to verify this similarity in the quantitative distribution of synapses between CO-rich and -poor regions, another series of electron micrographs was taken parallel to the cortical surface from layer III of one monkey (animal C). This lamina was chosen on the basis of the clear separation of CO-rich blob and CO-poor interblob regions. Two CO-rich and two CO-poor regions were analyzed in these tangential sections. The number, length, and distribution of GABA(+) synapses on different postsynaptic elements were not significantly different (ANOVA) between these two regions (Table 1, section C). Therefore, all subsequent values given in this article were from the pooled data calculated from CO-rich and -poor regions in the three monkeys studied and of another monkey (animal B) in which this distinction was not made.

### *Number of Neurons*

The average numerical densities of the total population and of GABA(+) neurons are shown in Table 2 and Figure 3. These estimates were calculated with the disector method. The two quantification methods provided results differing only by 3–5%. We decided to present data obtained with the disector method because it was not affected by the shape and the size–frequency distribution of the measured test objects. For the total cortical thickness (layers I–VI), the average numerical density of the total population of neurons was 114,800 ± 5200/mm³. Of these, 20.5% were considered to be GABA(+), corresponding to 23,600 neurons/mm³. GABA(−) neurons represent 79.5% of cortical neurons, corresponding to a numerical density of 91,200 neurons/mm³. There are considerable variations in the packing density of neurons among different cortical laminae. Low densities of neurons are evident in layers I, lower half of VI, IVB, V, and upper half of IVC as compared to their immediate neighbors. The packing densities of GABA(+) neurons follow a similar pattern of distribution, except that the difference between layer I and the other cortical laminae was smaller. Similarity of laminar variation between the $N_v$ of the overall population and of GABA(+) neurons results in a low variation in the proportion of GABA(+) neurons among the cortical laminae, with the notable exception of layer I in which the proportion reaches 85.2%. In other layers, the percentage of GABA(+) neurons ranges from 15.4% (upper part of layer VI) to 25.1%

**Table 2**
Number ($\times 10^3$) of neurons in area 17 of the monkey

| | Neurons/mm³ | | Neurons under 1 mm² of pia | | |
|---|---|---|---|---|---|
| Layers | All | GABA(+) | All | GABA(+) | % GABA(+) |
| I | 13.5 ± 9.9 | 11.5 ± 8.4 | 1.5 ± 1.1 | 1.2 ± 0.9 | 85.2 ± 10.5 |
| II-III, 1 | 151.8 ± 31.0 | 33.6 ± 19.6 | 30.8 ± 3.6 | 6.3 ± 2.1 | 20.9 ± 8.1 |
| II-III, 2 | 102.2 ± 18.9 | 22.8 ± 8.5 | 21.4 ± 5.9 | 4.5 ± 0.8 | 22.1 ± 6.5 |
| II-III | 127.0 ± 19.1 | 28.2 ± 14.0 | 52.1 ± 7.9 | 10.8 ± 2.9 | 21.2 ± 7.1 |
| IVA | 204.1 ± 26.4 | 44.5 ± 12.2 | 18.9 ± 2.8 | 4.3 ± 1.5 | 23.0 ± 9.2 |
| IVB | 96.2 ± 15.1 | 20.4 ± 4.6 | 17.7 ± 2.6 | 3.8 ± 0.9 | 21.3 ± 3.0 |
| IVC, 1 | 131.1 ± 9.3 | 21.8 ± 8.0 | 19.2 ± 2.3 | 3.1 ± 0.7 | 16.6 ± 5.7 |
| IVC, 2 | 186.9 ± 22.0 | 32.9 ± 4.8 | 27.5 ± 4.5 | 4.9 ± 1.2 | 17.7 ± 2.6 |
| IVC | 156.9 ± 15.7 | 27.0 ± 2.0 | 46.1 ± 7.0 | 7.9 ± 0.5 | 17.3 ± 1.8 |
| V | 92.8 ± 23.4 | 22.3 ± 6.4 | 10.9 ± 1.1 | 2.8 ± 0.9 | 25.1 ± 7.0 |
| VI, 1 | 138.0 ± 24.5 | 21.6 ± 5.9 | 19.1 ± 3.2 | 3.0 ± 0.7 | 15.4 ± 2.6 |
| VI, 2 | 52.2 ± 17.7 | 11.4 ± 0.4 | 7.6 ± 3.9 | 1.6 ± 0.4 | 24.8 ± 9.6 |
| VI | 97.1 ± 18.6 | 16.5 ± 2.9 | 27.2 ± 6.8 | 4.6 ± 0.9 | 17.1 ± 1.3 |
| I-VI | 114.8 ± 5.2 | 23.6 ± 3.8 | 174.4 ± 3.0 | 35.3 ± 20.4 | 20.5 ± 3.3 |

Data are means and SEM values ($n = 4$). 1, upper half; 2, lower half.

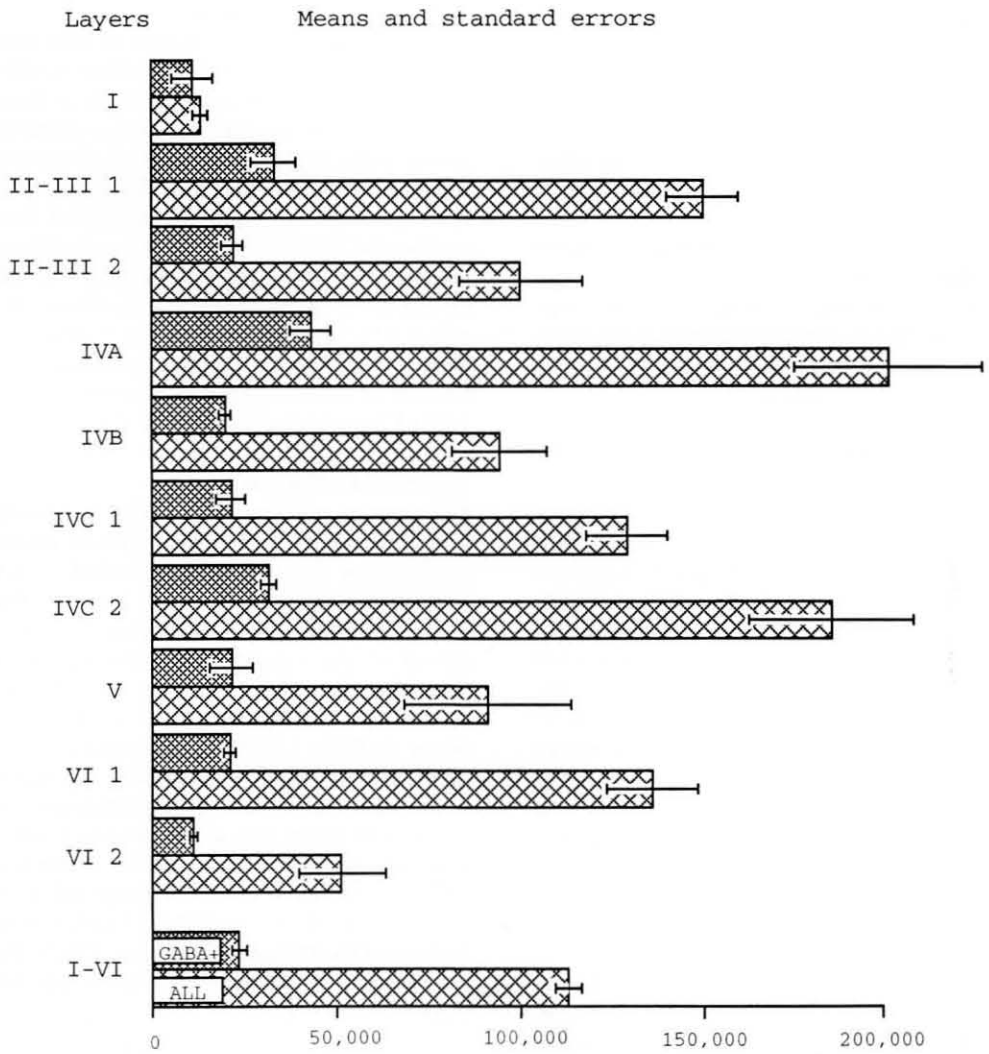


**Figure 3.** Number of GABA(+) and of the overall population of neurons per cubic millimeter of tissue in striate cortex of the monkey. Means and SEM values are given for the total cortical thickness (*I–VI*) and for each cortical lamina [layers *I*, upper half (*1*) and lower (*2*) half of *II-III, IVA, IVB*, upper and lower halves of *IVC, V*, and upper and lower halves of *VI*]. These numbers were obtained using the disector method.

**Table 3**
Numerical density ($\times 10^6$) and synapse-to-neuron ratio in different laminae of area 17 of monkeys

| | Synapses/mm³ | | Synapse-to-neuron ratio | | |
|---|---|---|---|---|---|
| Layers | All | GABA(+) | All | GABA(+) | % GABA(+) |
| I | 503.5 ± 57.5 | 115.8 ± 5.5 | 37,367 ± 2157 | 8594 ± 532 | 23.0 ± 3.4 |
| II-III | 539.6 ± 18.9 | 93.9 ± 4.2 | 4248 ± 420 | 739 ± 81 | 17.4 ± 8.3 |
| IVA | 489.0 ± 40.3 | 102.2 ± 3.6 | 2396 ± 192 | 501 ± 53 | 20.9 ± 9.0 |
| IVB | 430.4 ± 48.2 | 87.8 ± 4.2 | 4473 ± 251 | 912 ± 102 | 20.4 ± 3.4 |
| IVC | 451.8 ± 49.5 | 115.7 ± 3.8 | 2879 ± 206 | 737 ± 62 | 25.6 ± 5.3 |
| V | 434.4 ± 90.2 | 70.4 ± 5.6 | 4681 ± 513 | 758 ± 82 | 16.2 ± 3.7 |
| VI | 262.5 ± 34.7 | 49.7 ± 7.7 | 2703 ± 199 | 511 ± 51 | 18.9 ± 1.5 |
| I–VI | 445.7 ± 27.6 | 75.8 ± 5.3 | 3883 ± 293 | 660 ± 65 | 17.0 ± 1.6 |

Data are means and SEM values ($n = 4$).

(layer V); an estimate of 20.5% was calculated for the total cortical thickness (Table 1).

By combining laminar thickness and $N_V$, we determined the number of neurons in each lamina under 1 mm² of cortical surface. These figures for the overall population and for GABA(+) neurons were given in Table 2. For the total cortical thickness, there were about 174,400 neurons in a column of striate cortex beneath 1 mm² of pial surface. Supragranular laminae (layers I–II-III) contain 31% and granular laminae (layers IV) contain 47% of the total neurons in a column of visual cortex. The neurons in infragranular laminae represent 22% of the total population of neurons in a column of area 17. The distribution of the 20.5% of neurons that were GABA(+) among the laminae does not appreciably differ from that described for the total population of neurons: 34% (12,000) are located in the supragranular laminae, 45% (16,000) are in granular, and 21% (7400) are found in infragranular laminae.

### *The Number of All Synapses per Cubic Millimeter of Cortex*

The total number of synapses per cubic millimeter of tissue is given in Table 3, for each lamina and for the total cortical thickness. These estimates were obtained with the $N_A/d$ method (see Materials and Methods and Discussion). For the total cortical depth (layers I–VI), the numerical density of all synapses was in the order of 446 ± 28 million/mm³ of visual cortex. The average values obtained for the four monkeys are relatively uniform, the SEM expressed as a percentage of the mean (which is a good estimate of the sample variability) being in the order of 6%. The numbers of synapses/mm³ are similar from layer I to layer V (ranging from 434 million/mm³ in layer V to 539 million/mm³ in layer II-III), but in layer VI the $N_V$ is lower, probably due to the gradual increase of nonsynaptic axons.

In animal A, the total number of synapses was estimated by the disector method. With this technique, the numerical density of synapses for the total cortical depth (I–VI) was 451 million/mm³ compared to 410 million/mm³ using the $N_A/d$ formula in the same animal, resulting in a difference of only 9.1% between the two methods. However, a greater variation was found from layer to layer, probably because of the difficulty in recognizing disappearing synaptic contacts (see Discussion).

### *The Number of GABA(+) and GABA(−) Synapses/mm³ of Cortex*

For the total cortical thickness (I–VI), there are 76 million GABA(+) and 370 million GABA(−) synapses/mm³ of striate cortex (Table 3, Fig. 4). SEM values expressed as the percentage of the mean were in the order of 7% for GABA(+) and for GABA(−) synapses. This indicates that the $N_V$ values are similar among the four animals. In individual laminae, the number of GABA(+) synapses varied from 50 million/mm³ in layer VI to 118 million/mm³ in layer IVC (Table 3). Of the identified population of synapses, about 17% of all contacts were GABA(+) and 83% were GABA(−) for the total cortical thickness. In individual laminae, GABA(+) contacts ranged from 16% in layer V to 26% in layer IVC (Table 3).

### *Synapses to Neuron Ratios*

The average number of synapses per neuron is presented in Table 3 and Figure 5. These estimates were obtained by dividing the numerical density of synapses by the $N_V$ of neuronal cell bodies. It is important to note here that since these two estimates were obtained on the same material, the shrinkage did not affect this ratio. For the total cortical thickness, there were about 3900 synapses per neuron, 660 of them being GABA(+). There were variations among cortical layers, but it should be noted that many synapses in any given layer can be on processes of neurons whose cell body lies in a different layer. The total synapses to neuron ratio is the highest in layer I (37,400) and close to the average value in layers V (4700), IVB (4500), and II-III (4200). It was lowest in layers IVA, IVC, and VI (about 2500). The laminar distribution of GABA(+) synapses per neuron followed a similar pattern.

### *Length of Synaptic Thickening*

The mean cut length of the overall population (0.29 μm) and of the GABA(−) synapses (0.30 μm) was

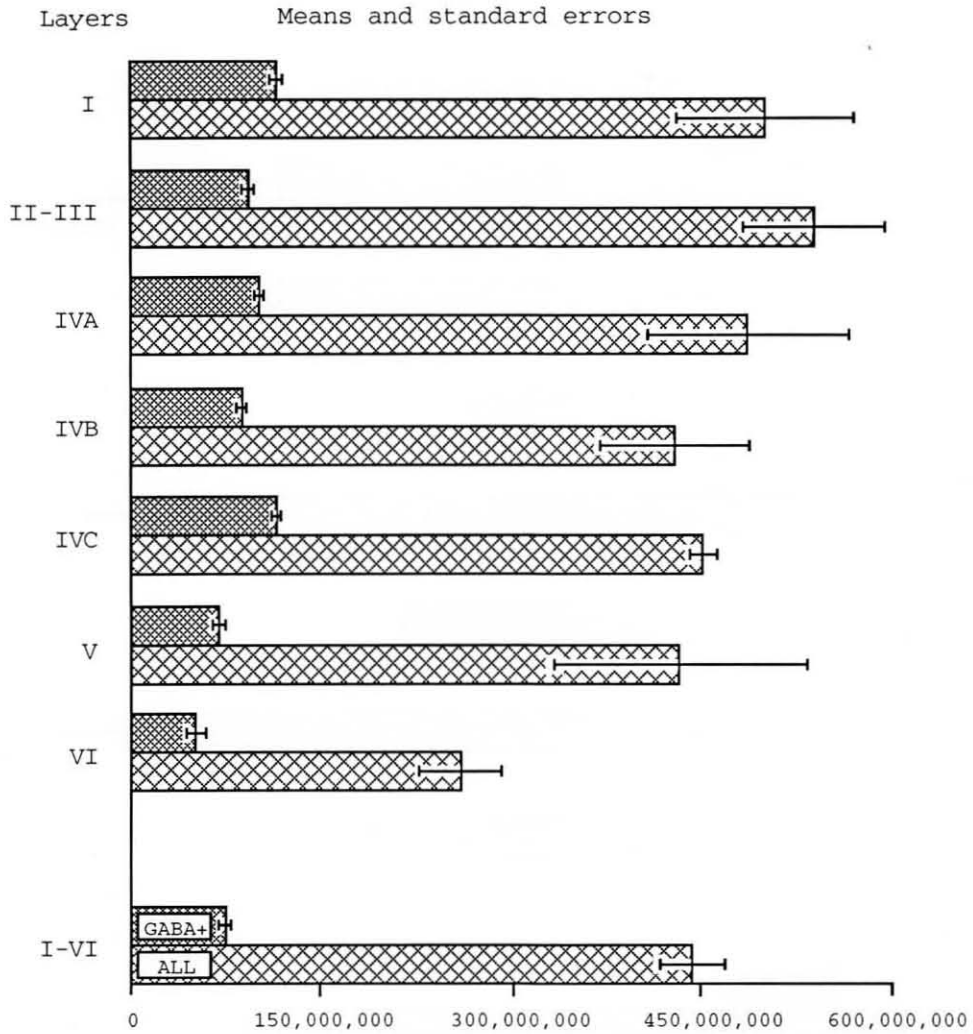


**Figure 4.** Number of GABA(+) and of the overall population of synapses per cubic millimeter of tissue in striate cortex of the monkey. Means and SEM values are given for the total cortical thickness (*I–VI*) and for each cortical lamina (layers *I, II-III, IVA, IVB, IVC, V,* and *VI*). These numbers were obtained using the $N_A/d$ method.

greater than that of the GABA(+) synapses for the total cortical thickness (0.24 $\mu$m). Synaptic length tends to be similar among cortical laminae. It appears, however, that the average lengths of GABA(+) and GABA(−) synapses on spines were greater (0.27 and 0.32 $\mu$m) than those obtained on dendrites (0.24 and 0.29 $\mu$m) or on somata (0.15 and 0.26 $\mu$m). This trend was present in all four monkeys studied.

### *Postsynaptic Elements*

The distribution of GABA(+) and GABA(−) synapses on spines, dendritic trunks, somata, and axon initial segments is given in Tables 4 and 5 and in Figures 6 and 7. Of the identifiable postsynaptic elements, 26.7% of GABA(+) synapses targeted spines, 61.6% were on dendrites, 11.7% were found on somata, and less than 0.1% contacted axon initial segments. Of these targets, 9.6% were GABA(+) (8.8% dendrites and 0.8% somata). From these proportions, we estimated[1] that there were about 20 million/mm$^3$ GABA(+) synapses on dendritic spines, 47 million/mm$^3$ on dendritic trunks, 9 million/mm$^3$ on somata, and 0.07 million/mm$^3$ on axon initial segments. In individual laminae, the proportion of GABA(+) synapses on spines and dendrites was similar to that obtained for the total cortical thickness. The percentages on somata and axon initial segments, however, varied greatly among the cortical laminae, perhaps reflecting the relatively low numbers of sampled synapses contacting the cell bodies. Only eight synaptic profiles out of a total sampling of about 6000 profiles involved axon initial segments in the four monkeys analyzed. Since they represent only a small proportion of the overall population of postsynaptic elements, we added their proportion to that of somata.

The target distribution of the GABA(−) synapses was different from that of GABA(+) synapses. For the total cortical thickness, the majority of GABA(−) synaptic contacts were found on spines (63.6%), fewer were found on dendrites (36.0%), and only a small proportion were on somata (0.5%). Of these targets, 9.6% were GABA(+) (9.1% on dendrites, 0.5% on somata). We have estimated (see note 1) that in 1 mm$^3$ of monkey visual cortex there were about 235

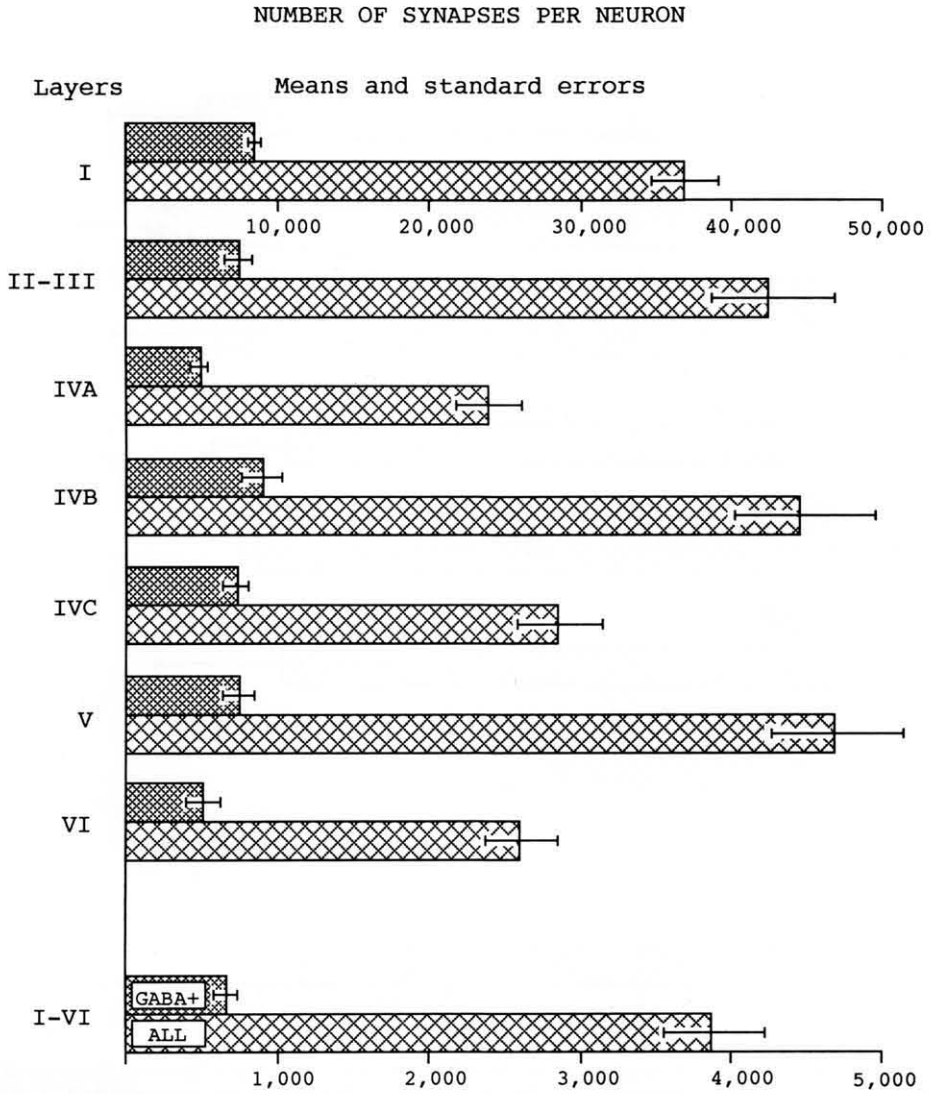


**Figure 5.** Number of GABA(+) and of the overall population of synapses per neuron in striate cortex of the monkey. Means and SEM values are given for the total cortical thickness (*I–VI*) and for each cortical lamina (layers *I, II-III, IVA, IVB, IVC, V,* and *VI*). These numbers were obtained by dividing the $N_v$ of synapses by the neuronal $N_v$.

million GABA(−) synapses on spines, 133 million on dendrites, and 2 million on somata. It should be noted that all somata targeted by GABA(−) synapses were GABA(+). In individual laminae, the proportion of GABA(−) synapses on spines and dendrites remains relatively constant.

### *Correlation between the Structure and GABA Reactivity of Synaptic Terminals*

Synaptic contacts in which the synaptic cleft could be seen unambiguously ($n = 406$) were evaluated in area 17. Of these, 349 synapses were classified as type 1 or asymmetric, 44 were type 2 or symmetric, and the extent of the postsynaptic membrane specializa-

**Table 4**
Percentage of GABA(+) synapses on spines, dendrites, and somata and axon initial segments

| Layers | Spines | Dendrites | Somata and axon initial segments |
|---|---|---|---|
| I | 27.9 (0) | 72.1 (5.7) | 0 (0) |
| II-III | 28.3 (0) | 54.2 (11.4) | 17.5 (0) |
| IVA | 27.8 (0) | 56.3 (10.3) | 15.9 (3.6) |
| IVB | 24.1 (0) | 67.8 (7.9) | 8.1 (0) |
| IVC | 24.9 (0) | 57.6 (6.3) | 17.5 (4.6) |
| V | 37.8 (0) | 72.2 (9.7) | 0 (0) |
| VI | 25.8 (0) | 74.2 (4.1) | 0 (0) |
| I–VI | 26.7 (0) | 61.6 (8.8) | 11.7 (0.8) |

Numbers in parentheses are proportions on GABA(+) postsynaptic elements ($n = 4$).

**Table 5**
Percentage of GABA(−) synapses on spines, dendrites, and somata

| Layers | Spines | Dendrites | Somata |
|---|---|---|---|
| I | 57.4 (0) | 42.6 (14.7) | 0 (0) |
| II-III | 66.5 (0) | 33.5 (10.1) | 0 (0) |
| IVA | 59.9 (0) | 36.6 (8.6) | 3.5 (3.5) |
| IVB | 61.0 (0) | 36.6 (8.6) | 2.4 (2.4) |
| IVC | 56.8 (0) | 42.6 (6.0) | 0.6 (0.6) |
| V | 68.3 (0) | 31.7 (8.8) | 0 (0) |
| VI | 69.0 (0) | 31.0 (8.2) | 0 (0) |
| I–VI | 63.6 (0) | 35.9 (9.1) | 0.5 (0.5) |

Numbers in parentheses are proportions on GABA(+) postsynaptic elements ($n = 4$).

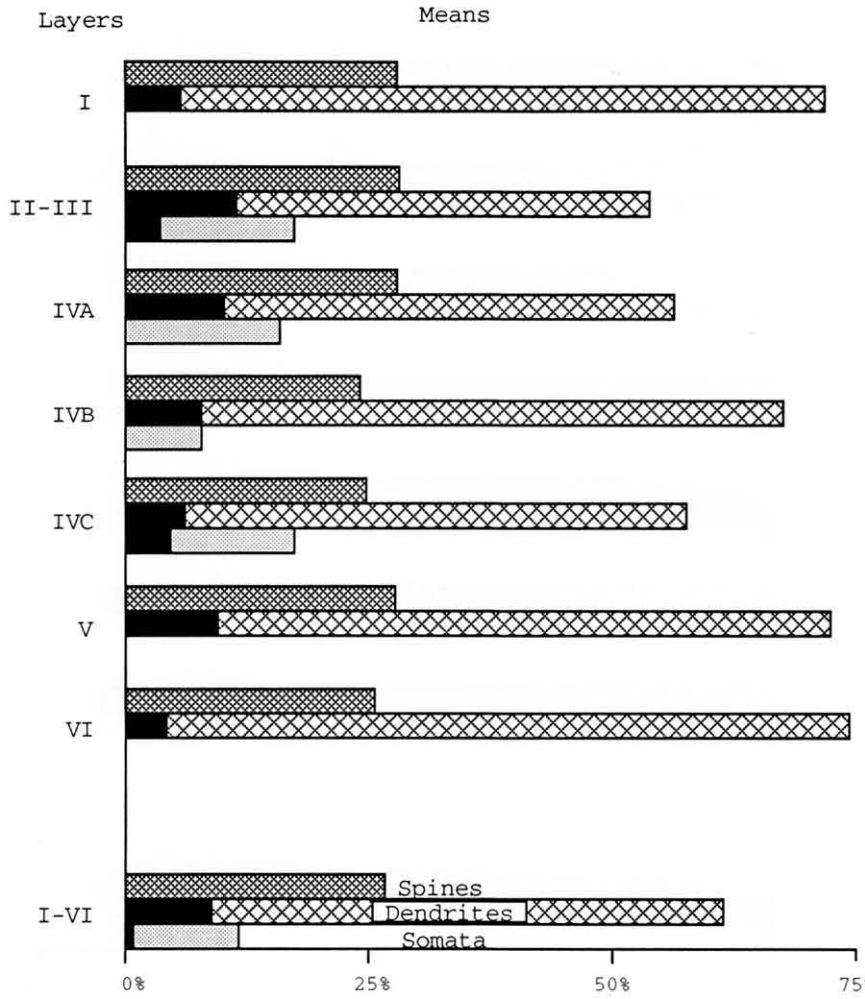


**Figure 6.** Distribution of postsynaptic targets to GABA(+) synapses in each lamina in area 17 of the monkey cortex. *Solid bars* represent the proportion of GABA(+) postsynaptic elements.

tions was equivocal at 13 synapses. The vast majority of terminals showing asymmetric synapses (345 out of 349; 98.9%) were GABA(−). The GABA immunoreactivity of the four remaining asymmetric synapses was equivocal.

Among the 44 symmetric synapses examined, 42 (95.5%) were clearly GABA(+). Two symmetric synapses were placed in the "undetermined" category due to equivocal GABA reactivity over these profiles.

In addition to the correlation between the extent of the postsynaptic specialization and the GABA immunoreactivity of the presynaptic terminal, the shape of the synaptic vesicles was also analyzed qualitatively. In 319 out of the 406 terminals, the shape of the synaptic vesicles could be determined unambiguously. All terminals with asymmetric synapses contained round vesicles, and all terminals with symmetrical contacts contained small pleomorphic synaptic vesicles (see Fig. 2).

## Discussion

### *Accuracy of Absolute Values*

Some of the stereological methods used in the present study rely on assumptions about the shape and the size–frequency distribution of the objects being measured. Unbiased stereological methods recently introduced by Sterio (1984; see review by Gundersen et al., 1988a,b) are not dependent on assumptions about shape and distribution. It has been proposed that these methods are more reliable than those based on rough approximation of the shape. In the present study, we applied the disector method for the determination of the number of GABA(+) neurons and, in one animal, for the determination of the number of synapses. We found, as described previously by others (Pakkenberg and Gundersen, 1988; West et al., 1988; Braendgaard et al., 1990; Mayhew, 1991), that the disector method has several advantages over conventional methods for the determination of the number of neurons. These advantages range from being less time consuming to the relative simplicity of applying the method. However, there were practical problems in applying the method to synapses. In our hands, it was more time consuming and more difficult to apply than the $N_A/d$ method, for the following reasons. When using two consecutive ultrathin sections (60–80 nm thick), the number of synaptic profiles disappearing ($Q-$ in the disector formula) on the next section is low. Therefore, in order to increase

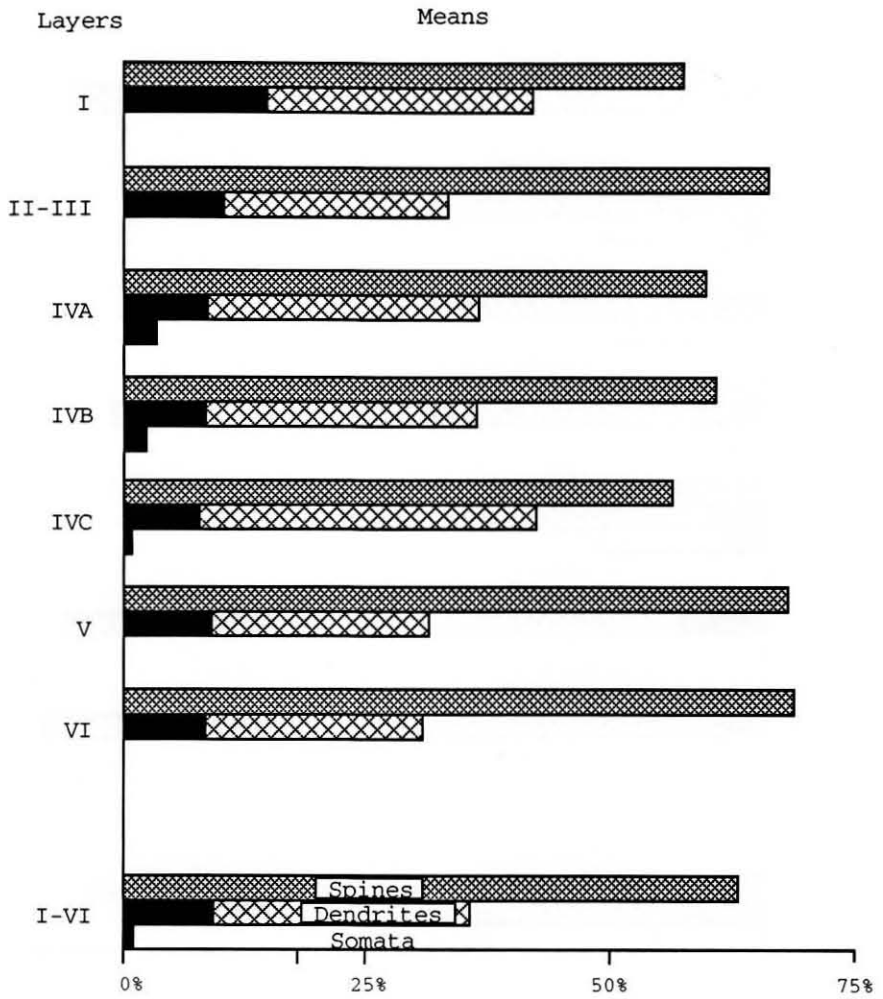


**Figure 7.** Distribution of postsynaptic targets to GABA(−) synapses in each lamina in area 17 of the monkey cortex. *Solid bars* represent the proportion of GABA(+) postsynaptic elements.

this number, especially if several categories of synapses were analyzed, the sampling area must be considerably increased. Moreover, the sampling was based on those synaptic junctions so small in size that they disappeared in the next ultrathin section. These were the most difficult synapses to identify and characterize. A reasonable compromise is to cut more serial sections or to analyze more distant sections. With the $N_A/d$ method, all synapses were sampled in the test area, and the above problems became less crucial. Thus, although this stereological method relies on rough assumptions of the shape and distribution of objects, errors introduced should be less than 10% (Colonnier and Beaulieu, 1985).

Our results were based on the selective detection of GABA in neuronal elements using the postembedding immunogold technique. We achieved strong immunoreactivity over a select population of elements (terminals, dendrites, and somata; see Fig. 2) with low levels of immunogold elsewhere. As in all immunocytochemistry, it is not possible to determine whether all GABA(+) elements were labeled, because some structures may have GABA levels below the sensitivity of our method. It should be noted, however, that one of the major problems in immunological techniques, the penetration of the antibody into the tissue, is overcome by the postembedding techniques, since the reaction was located on the surface of the section.

Interestingly, the density of gold particles over dendritic profiles was consistently lower than that found over nerve terminals. Furthermore, and in agreement with previous reports, the level of GABA immunostaining was often highest over mitochondria. Since GABA is actually metabolized by mitochondrial enzymes, the high immunoreactivity over mitochondria indicates high concentration of GABA in these cell organelles, which makes the classification of the profiles easier. However, small dendrites or spines that do not contain mitochondria but originate from GABAergic cells may not show immunostaining for GABA and may be falsely classified as GABA(−). Therefore, we cannot rule out the possibility that some GABAergic nerve terminals and especially some dendrites were considered as GABA(−) or placed in the category equivocal for GABA reactivity. As mentioned in Materials and Methods, the number of synapses in this latter category was added

proportionally to GABA(+) synapses. If these equivocally labeled synapses were all GABA(+), our numerical results may be somewhat biased toward underestimating the GABA(+) neuronal elements. However, the bias will not be great because this category of synapses represents only 2.6 ± 1.1% of the total population.

### *Comparison between CO-Rich and -Poor Regions*

It has been suggested that the prominent CO zones of area 17 are also enriched in the amount of the GABA-synthesizing enzyme GAD (Hendrickson et al., 1981). Interestingly, however, a previous study (Hendry et al., 1987) found no difference in the number of GABA(+) neurons in CO-rich patches and in the CO-poor zones. The present study confirms and extends this finding as the quantitative distribution of GABA(+) neurons and nerve terminals was not different between CO-rich and CO-poor regions.

### *Morphology of GABA Terminals*

A strong correlation was found between the morphology of the synaptic vesicles, the extent of the postsynaptic opacity, and the presence of GABA immunoreactivity in axonal terminals. A similar correlation has been reported in the cat visual cortex (Beaulieu and Somogyi, 1990). In this latter species, however, in addition to terminals having pleomorphic vesicles and type 2 junctions, a second and small population of GABA(+) terminals containing large ovoid synaptic vesicles also made type 2 synaptic contacts. We did not find similar terminals in the monkey. It may be that the sample was not large enough to encounter them.

Terminals containing pleomorphic vesicles and making type 2 or symmetrical synapses have been assumed, without direct neurochemical evidence, to exert inhibitory influence (Gray, 1959; Uchizono, 1965; Szentagothai, 1969). Previous qualitative immunocytochemical studies (Ribak, 1978; Freund et al., 1983; for a review see Houser et al., 1984) and the present quantitative results largely support this assumption. It should be emphasized, however, that although many of the boutons forming symmetrical or type 2 synapses do indeed contain GABA in the cortex, the chemical nature of any individual bouton cannot be determined with certainty when based solely on morphological criteria. For example, dopaminergic (Goldman-Rakic et al., 1989) boutons also form type 2 synapses in the primate cortex. From our quantitative study, it is clear that the total contribution of these synapses is probably less than 5%.

### *Numerical Parameters of Cortical Circuitry*

There are many estimates of the numerical density of neurons in the striate cortex of monkeys (for a review, see Colonnier and O'Kusky, 1981). All agree that there are more neurons per unit volume of tissue in the striate cortex of primates than in other cortical areas or in the neocortex of nonprimate mammals. Is this difference reflected in the number of GABA neurons? In the cat (Gabbott and Somogyi, 1986) and in the monkey, 20% of the total population of visual cortical neurons were GABA(+). Since there were 2.5 times more neurons per unit volume in the monkey visual cortex, the absolute number of GABA(+) neurons is also 2.5 times higher in the monkey. Comparing different cortical areas in the monkey cortex, Hendry et al. (1987) have also estimated that the visual cortex contains more GABA(+) neurons beneath a given pial surface than any other cortical area. The explanation for or consequences of the high number of neurons in primates is still under debate, but it appears that as more neurons are added to cortex, the basic cortical circuit retains the same proportion of inhibitory neurons.

As reported in the cat (Gabbott and Somogyi, 1986), rat (Meinecke and Peters, 1987), and monkey (Hendry et al., 1987), the vast majority of neurons in layer I are GABA(+). This layer has the lowest numerical density of neurons while the density of synapses was about the same as in other layers, but most of these synapses are on processes originating from other layers.

We calculated the overall number of synapses to be 446 million/mm$^3$ of the monkey striate cortex, providing on average 3900 synapses/neuron. These estimates are higher than those calculated by O'Kusky and Colonnier (1982; 276 million/mm$^3$ and 2300 synapses/neuron). The difference between our estimates and those of O'Kusky and Colonnier can be attributed largely to the different formulas used in these two studies. They used a formula that tends to underestimate the synaptic number (see Colonnier and Beaulieu, 1985). Using our formula, the overall number of synapses reported by O'Kusky and Colonnier would increase by some 50%, resulting in a value of 414 million/mm$^3$ and 3450 synapses per neuron, close to the values obtained in the present study.

Having obtained estimates for the monkey, comparison can be made among the most frequently studied species in the parameters of inhibitory synaptic connections. In the striate cortex of monkey, 76 million of the 446 million synapses/mm$^3$ (17%) are GABA(+). In cat visual cortex, it has been estimated (Beaulieu and Colonnier, 1985b; Beaulieu and Somogyi, 1990) that 48 million of the 286 million synapses/mm$^3$ of tissue were GABA(+) (17%). Even though the numerical density of synapses in the cat visual cortex is only two-thirds of that calculated in the monkey, the similar proportion of GABA(+) synapses in these two species is remarkable. Also, a similar proportion of synapses was GABA(+) throughout the layers, and this supports the notion that a basic cortical circuit is repeated from layer to layer and species to species.

It would be interesting to compare these parameters to those of the rat, used extensively in cortical studies. There does not exist, to our knowledge, any direct estimate of the quantitative distribution of GABA(+) synapses in the rat visual cortex. Peters and Feldman (1976; see also Peters, 1987) reported that symmetrical synapses accounted for 13% of the total population of synapses in layer IV. Assuming that most

of these were GABA(+) synapses, the proportion appears somewhat lower in this species than in cats and monkeys.

The numerical parameters of cortical circuitry can be compared among species using the present and published data, provided the methods in different studies are comparable. The neuronal density was higher in the monkey (115,000/mm$^3$) than in the cat (50,000/mm$^3$; Beaulieu and Colonnier, 1983) or in the rat visual cortex (80,000/mm$^3$; Warren and Bedi, 1982; Peters, 1987). The number of GABA(+) synapses was estimated to be 76 million/mm$^3$ in the monkey, 48 million/mm$^3$ in the cat, and 100–125 million/mm$^3$ in the rat (13% of symmetrical synapses from a total population of 750–950 million/mm$^3$; Warren and Bedi, 1982; Peters, 1987). From these data, the number of GABA(+) synapses per neuron can be estimated for these species. It transpires that an "average" neuron in the monkey visual cortex receives fewer GABA(+) synaptic contacts (660) than the cat (960), or the rat (1250–1560). A similar trend can be detected for the GABA(−) synapses. The monkey has the smallest number of GABA(−) synapses/neuron (3200), followed by the cat (4900) and the rat (11,000). This suggests that an "average" neuron in the monkey cortex integrates fewer inputs, and may indicate a progressive specialization of neurons processing a restricted range of visual information. Assuming that each neuron represents a separate analytical channel, fewer inputs from different sources could increase the efficacy of the system, resulting in a speedier extraction of more aspects of sensory information. However, in addition to the numbers, the localization of the impinging synapses on the recipient neuron may also contribute to the characteristics of processing carried out by the cell.

### *Postsynaptic Targets of Synaptic Terminals*

The distribution of the targets of GABA(+) synapses can predict quantitatively the sites of GABAergic influences in cortex. It emerges that the major targets of GABA(+) synapses are dendritic shafts and spines, which together comprised 88% of the postsynaptic elements. From this result, it is clear that most of the GABA inhibition in cortex takes place on the dendritic processes of the cells in interaction with other inputs to the neuron. This is well illustrated by the finding that about every fourth GABA(+) synapse was devoted to dendritic spines, receiving one excitatory and one inhibitory synapse in most cases (e.g., Fig. 2*C*). Furthermore, neuronal somata were only half as likely to be targets of GABA(+) synapses as spines. GABA(−) synapses also targeted mainly dendritic spines and dendritic trunks, but these synapses were more often on dendritic spines rather than on dendritic trunks.

Neurons that contain GABA comprised 20% of all neurons in the striate cortex of monkey. If GABAergic and non-GABAergic cells received, on average, the same number of synapses from GABA(+) terminals, one would expect that 20% of all postsynaptic targets were also GABA(+). Only 9.6% of GABA(+) synapses targeted GABA(+) elements [8.8% on GABA(+) dendrites and 0.8% on GABA(+) cell bodies]. This means that 14% of the dendrites and 7% of the cell bodies being targeted by GABA(+) synapses were GABA(+). A similar calculation for GABA(−) synapses also showed fewer synapses on GABA(+) targets than expected from the overall proportion of cells. Thus, either our method did not reveal all the GABAergic dendrites or, on average, GABAergic neurons received fewer synapses on their dendrites or cell bodies than did non-GABAergic cortical cells. These alternatives are currently under study.

## Notes

We are grateful to Mrs. Claire Crevier and to Mr. Frank Kennedy for their excellent technical and photographic assistance. The work was supported by the Medical Research Council of Canada (C.B. and M.C.) and of Great Britain (P.S. and A.C.) and by grants from Fonds de la Recherche en Santé du Québec (C.B.) and of the Fonds de Développement de la Recherche de l'Université de Montréal (C.B.).

Correspondence can be addressed to any of the authors.

Present address of Z.K. is Ruhr-Universitat Bochum, Medizinische Fakultat, Department of Neurophysiology, Universitatsstrasse 150, D-4630, Bochum 1, Germany.

1. The number of synapses on each category of postsynaptic element was calculated as the total number of synapses divided according to the percentage of the identifiable postsynaptic elements, assuming that the distribution of the unidentified elements was the same as those found for the identified targets.

## References

Beaulieu C, Colonnier M (1983) The number of neurons in the different laminae of the binocular and monocular regions of area 17 in the cat. J Comp Neurol 217:337–344.

Beaulieu C, Colonnier M (1985a) A comparison of the number of neurons in individual laminae of cortical areas 17, 18, and posteromedial suprasylvian (PMLS) in the cat. Brain Res 339:166–170.

Beaulieu C, Colonnier M (1985b) A laminar analysis of the number of round-asymmetrical and flat-symmetrical synapses on spines, dendritic trunks, and cell bodies in area 17 of the cat. J Comp Neurol 231:180–189.

Beaulieu C, Somogyi P (1990) Targets and quantitative distribution of GABAergic synapses in the visual cortex of the cat. Eur J Neurosci 2:296–303.

Braendgaard H, Evans SM, Howard CV, Gundersen HJG (1990) The total number of neurons in the human neocortex unbiasedly estimated using optical disectors. J Microsc 157:285–304.

Cohen RS, Siekevitz P (1978) Form of the postsynaptic density. A serial section study. J Cell Biol 78:36–46.

Colonnier M, Beaulieu C (1985) An empirical assessment of stereological formulae applied to the counting of synaptic disks in the cerebral cortex. J Comp Neurol 231: 175–179.

Colonnier M, O'Kusky J (1981) Le nombre de neurones et de synapses dans le cortex visuel de différentes espèces. Rev Can Biol 40:91–99.

Dykes RW, Landry P, Metherate R, Hicks TP (1984) Functional role of GABA in cat primary somatosensory cortex: shaping receptive fields of cortical neurons. J Neurophysiol 52:1066–1093.

Freund TF, Martin KAC, Smith AD, Somogyi P (1983) Glutamate decarboxylase-immunoreactive terminals of Golgi-impregnated axoaxonic cells and of presumed basket cells in synaptic contact with pyramidal neurons of the cat's visual cortex. J Comp Neurol 221:263–278.

Gabbott PLA, Somogyi P (1986) Quantitative distribution

of GABA-immunoreactive neurons in the visual cortex (area 17) of the cat. Exp Brain Res 61:323–331.
Goldman-Rakic PS, Leranth C, Williams SM, Mons N, Geffard M (1989) Dopamine synaptic complex with pyramidal neurons in primate cerebral cortex. Proc Natl Acad Sci USA 86:9015–9019.
Gray EG (1959) Axo-somatic and axo-dendritic synapses of the cerebral cortex: an electron microscope study. J Anat 93:420–433.
Gundersen HJG, Bendtsen TF, Korbo L, Marcussen N, Moller A, Nielsen K, Nyengaard JR, Pakkenberg B, Sorensen FB, Vesterby A, West MJ (1988a) Some new, simple and efficient stereological methods and their use in pathological research and diagnosis. Acta Pathol Microbiol Scand [C] 96:379–394.
Gundersen HJG, Bagger P, Bendtsen TF, Evans SM, Korbo L, Marcussen N, Moller A, Nielsen K, Nyengaard JR, Pakkenberg B, Sorensen FB, Vesterby A, West MJ (1988b) The new stereological tools: disector, fractionator, nucleator and point sampled intercepts and their use in pathological research and diagnosis. Acta Pathol Microbiol Scand [C] 96:857–881.
Hendrickson AE, Hunt SP, Wu J-Y (1981) Immunocytochemical localization of glutamic acid decarboxylase in monkey striate cortex. Nature 292:605–607.
Hendry SHC, Schwark HD, Jones EG, Yan J (1987) Numbers and proportions of GABA-immunoreactive neurons in different areas of monkey cerebral cortex. J Neurosci 7:1503–1519.
Hodgson AJ, Penke B, Erdei A, Chubb IW, Somogyi P (1985) Antiserum to γ-aminobutyric acid. I. Production and characterization using a new model system. J Histochem Cytochem 33:229–239.
Houser CR, Vaughn JE, Hendry SHC, Jones EG, Peters A (1984) GABA neurons in the cerebral cortex. In: Cerebral cortex, Vol 2, Functional properties of cortical cells (Jones EG, Peters A, eds), pp 63–89. New York: Plenum.
Kisvarday ZF, Cowey A, Somogyi P (1986) Synaptic relationship of a type of GABA-immunoreactive neuron (clutch cell), spiny stellate cells and lateral geniculate nucleus afferents in layer IVC of the monkey striate cortex. Neuroscience 19:741–761.
Krnjevic K (1984) Neurotransmitters in cerebral cortex: a general account. In: Cerebral cortex, Vol 2, Functional properties of cortical cells (Jones EG, Peters A, eds), pp 39–61. New York: Plenum.
Lund JS, Boothe RG (1975) Interlaminar connections and pyramidal neuron organization in the visual cortex, area 17, of the macaque monkey. J Comp Neurol 159:305–334.
Mayhew TM (1991) Accurate prediction of purkinje cell number from cerebellar weight can be achieved with the fractionator. J Comp Neurol 308:162–168.
Meinecke DL, Peters A (1987) GABA immunoreactive neurons in rat visual cortex. J Comp Neurol 261:388–404.
O'Kusky J, Colonnier M (1982) A laminar analysis of the number of neurons, glia, and synapses in the visual cortex (area 17) of adult macaque monkeys. J Comp Neurol 210: 278–290.
Pakkenberg B, Gundersen HJB (1988) Total number of neurons and glial cells in human brain nuclei estimated by the disector and the fractionator. J Microsc 150:1–20.
Peters A (1987) Number of neurons and synapses in primary visual cortex. In: Cerebral cortex, Vol 6, Further aspects of cortical function, including hippocampus (Jones EG, Peters A, eds), pp 267–294. New York: Plenum.
Peters A, Feldman ML (1976) The projection of the lateral geniculate nucleus to area 17 of the rat cerebral cortex. I. General description. J Neurocytol 5:63–84.
Peters A, Kaisermann-Abramof IR (1969) The small pyramidal neurons of the rat cerebral cortex. The synapses upon dendritic spines. Z Zellforsch Mikrosk Anat 100: 487–506.
Ribak CE (1978) Aspinous and sparsely-spinous stellate neurons in the visual cortex of rats contain glutamic acid decarboxylase. J Neurocytol 7:461–478.
Richardson KC, Jarret L, Hinke EH (1960) Embedding in epoxy resins for ultrathin sectioning in electron microscopy. Stain Technol 35:313–323.
Sillito AM (1975) The contribution of inhibitory mechanisms to the receptive field properties of neurons in the striate cortex of the cat. J Physiol (Lond) 250:305–329.
Sillito AM (1977) Inhibitory processes underlying the directional specificity of simple, complex and hypercomplex cells in cat's visual cortex. J Physiol (Lond) 271: 699–720.
Sillito AM, Kemp JA, Wilson JA, Berardi N (1980) A reevaluation of the mechanisms underlying simple cell orientation selectivity. Brain Res 194:517--520.
Silverman MS, Tootell RBH (1987) Modified technique for cytochrome oxidase histochemistry: increased staining intensity and compatibility with 2-deoxyglucose autoradiography. J Neurosci Methods 19:1–10.
Somogyi P, Hodgson AJ (1985) Antisera to γ-aminobutyric acid. III. Demonstration of GABA in Golgi-impregnated neurons and in conventional electron microscopic sections of cat striate cortex. J Histochem Cytochem 33:249–257.
Somogyi P, Hodgson AJ, Chubb IW, Penke B, Erdei A (1985) Antisera to γ-aminobutyric acid. II. Immunocytochemical application to the central nervous system. J Histochem Cytochem 33:240–248.
Sterio DC (1984) The unbiased estimation of number and sizes of arbitrary particles using the disector. J Microsc 134:127–136.
Szentagothai J (1969) Architecture of the cerebral cortex. In: Basic mechanisms of the epilepsies (Jasper HH, Ward AA Jr, Pope A, eds), pp 13–28. London: Churchill.
Uchizono K (1965) Characteristics of excitatory and inhibitory synapses in the central nervous system of the cat. Nature 207:642–643.
Warren MA, Bedi KS (1982) Synapse-to-neuron ratios in the visual cortex of adult rats undernourished from about birth until 100 days of age. J Comp Neurol 210:59–64.
Weibel ER (1979) Stereological methods, Vol 1, Practical methods for biological morphometry. London, Academic.
West MJ, Coleman PD, Flood DG (1988) Estimation the number of granule cells in the dentate gyrus with the disector. Brain Res 448:167–172.
Wong-Riley M (1979) Changes in the visual system of monocularly sutured or enucleated cats demonstrable with cytochrome oxidase histochemistry. Brain Res 171:11–28.